





# Geophysical Research Letters<sup>®</sup>



## RESEARCH LETTER

10.1029/2023GL106908

## Thermoelastic Properties of Fe<sup>3+</sup>-Rich Jeffbenite and Application to Superdeep Diamond Barometry

Fei Qin<sup>1</sup> , Fei Wang<sup>2</sup> , Joseph R. Smyth<sup>3</sup>, Dongzhou Zhang<sup>4</sup> , Jingui Xu<sup>5</sup>, and Steven D. Jacobsen<sup>6</sup> 

### Key Points:

- We measure the phase stability and thermoelastic properties on synthetic Fe-bearing jeffbenite
- The thermoelastic data are applied to modeling isomekes and the remnant pressure ( $P_{inc}$ ) is determined
- The smaller thermal expansivity of jeffbenite gives rise to a broader pressure and temperature stability field in the upper lower mantle

<sup>1</sup>School of Earth Sciences and Resources, China University of Geosciences (Beijing), Beijing, China, <sup>2</sup>Bayerisches Geoinstitut, Universiteit Bayreuth, Bayreuth, Germany, <sup>3</sup>Department of Geological Sciences, University of Colorado, Boulder, CO, USA, <sup>4</sup>School of Ocean and Earth Science and Technology, Hawai'i Institute of Geophysics and Planetology, University of Hawaii at Manoa, Honolulu, HI, USA, <sup>5</sup>Key Laboratory for High-Temperature and High-Pressure Study of the Earth's Interior, Institute of Chemistry, Chinese Academy of Sciences, Guiyang, China, <sup>6</sup>Department of Earth and Planetary Sciences, Northwestern University, Evanston, IL, USA

### Supporting Information:

Supporting Information may be found in the online version of this article.

### Correspondence to:

F. Qin and S. D. Jacobsen,  
fei.qin@cugb.edu.cn;  
s-jacobsen@northwestern.edu

### Citation:

Qin, F., Wang, F., Smyth, J. R., Zhang, D., Xu, J., & Jacobsen, S. D. (2024). Thermoelastic properties of Fe<sup>3+</sup>-rich jeffbenite and application to superdeep diamond barometry. *Geophysical Research Letters*, 51, e2023GL106908. <https://doi.org/10.1029/2023GL106908>

Received 1 NOV 2023  
Accepted 26 FEB 2024

**Abstract** Jeffbenite (Mg<sub>3</sub>Al<sub>2</sub>Si<sub>3</sub>O<sub>12</sub>) is a tetragonal phase found in so far only in superdeep diamonds, and its thermoelastic parameters are a prerequisite for determining entrapment pressures as it is regarded as a potential indicator for superdeep diamonds. In this study, the thermoelastic properties of synthetic Fe<sup>3+</sup>-jeffbenite were measured up to 33.7 GPa and 750 K. High-temperature static compression data were fitted, giving  $(\partial K_{T0}/\partial T)_P = -0.0107$  (4) GPa/K and  $\alpha_T = 3.50$  (3)  $\times 10^{-5}$  K<sup>-1</sup>. The thermoelastic properties and phase stability are applied to modeling isomekes, or  $P$ - $T$  paths intersecting possible conditions of entrapment in diamond. We calculate that under ideal exhumation, jeffbenite entrapped at mantle transition zone conditions will exhibit a high remnant pressure at 300 K ( $P_{inc}$ ) of  $\sim 5.0$  GPa. Elastic geobarometry on future finds of jeffbenite inclusions can use the new equation of state to estimate entrapment pressures for this phase with still highly uncertain stability field in the mantle.

**Plain Language Summary** Ongoing superdeep diamonds research is providing new insights into the Earth's deep mantle. Natural superdeep diamonds and its inclusions can show compelling evidence for retrograde conversion from the lower mantle or transition zone precursors; along with carbonate melt-peridotite reactions. Jeffbenite with a composition of Mg<sub>3</sub>Al<sub>2</sub>Si<sub>3</sub>O<sub>12</sub>, found in so far only in superdeep diamonds can be regarded as a potential indicator mineral for superdeep diamonds. Recent synthesis of Fe<sup>3+</sup>-rich jeffbenite provides an opportunity for in-situ measurements to study the thermodynamic properties of jeffbenite at deep-mantle conditions. Thus, in this study, we explored the high pressure and temperature stability and thermoelastic properties of Fe-bearing jeffbenite up to 33.7 GPa and 750 K. The thermoelastic data and phase stability were measured and the results are applied to modeling the isomekes, or  $P$ - $T$  paths intersecting possible conditions of entrapment and along which the pressure on the inclusion is equal to the external pressure on the diamond host. Our finding can be applied to determining entrapment pressures in such diamond inclusions in future finds and its primary or retrograde history is essential in understanding mantle dynamics and the hidden consequences of plate tectonics.

## 1. Introduction

Natural diamonds and their hosted inclusions provide unique insights into the Earth's deep mantle to at least  $\sim 1,000$  km depth (Nestola et al., 2018; Pearson et al., 2014; Shirey et al., 2013; Walter et al., 2011). Superdeep diamonds, from below 300-km depth, contain inclusions normally showing evidence for retrograde phase transitions from lower mantle or transition zone precursors, along with carbonate melt-peridotite reactions (Harte, 2010; Stachel et al., 2005; Thomson et al., 2016; Walter et al., 2008). Majoritic garnets are the only numerous inclusion population that largely retains its structure and chemical properties without retrograde re-equilibrations, and until now, the very high Fe<sup>3+</sup>/ $\Sigma$ Fe ratio ( $>0.8$ ) observed in high-pressure majoritic inclusions have revealed a much deeper orogenic carbonatite origin and redox states of the deep Earth (Kiseeva et al., 2018; Nestola, Regier, et al., 2023; Tao et al., 2018; Xu et al., 2017). However, in some superdeep diamonds, jeffbenite appears instead of majoritic garnet, especially from Brazil's Juina district and from Kankan in Guinea (Bulanova et al., 2010; Hayman et al., 2005; Hutchison et al., 2001; Zedgenizov et al., 2014, 2020). The

© 2024. The Authors.

This is an open access article under the terms of the [Creative Commons Attribution-NonCommercial-NoDerivs License](#), which permits use and distribution in any medium, provided the original work is properly cited, the use is non-commercial and no modifications or adaptations are made.

recent synthesis of Fe-rich jeffbenite with high Fe<sup>3+</sup> content by Smyth et al. (2022) provides an opportunity for laboratory experiments to study the thermodynamic properties of jeffbenite at deep-mantle conditions.

Prior to establishment as jeffbenite (Nestola et al., 2016), the tetragonal phase with ideal formula Mg<sub>3</sub>Al<sub>2</sub>Si<sub>3</sub>O<sub>12</sub> was referred to as TAPP (Tetragonal almandine-pyrope phase) (Harris et al., 1997) and is very similar to that of almandine-pyrope garnet compositions but with an unusual high ratio of Fe<sup>3+</sup>/(Fe<sup>2+</sup>+Fe<sup>3+</sup>) (Harris et al., 1997; McCammon et al., 1997). Thus, despite having garnet stoichiometry, TAPP was speculated to have its own stability field due to its lower density and modified crystal structure (Armstrong & Walter, 2012; Finger & Conrad, 2000; Harris et al., 1997; Smyth et al., 2022; Wang et al., 2021).

Recently, Nestola, Prencipe, and Belmonte (2023) calculated the phase diagram of jeffbenite from its thermodynamic properties and using density functional theory, predicting that pyrope should be stable over jeffbenite at mantle conditions. Given that the study of Nestola, Prencipe, and Belmonte (2023) was performed on Mg-end member jeffbenite and the conditions of synthesis at 15 GPa and 1,200°C for ferromagnesian jeffbenite (Smyth et al., 2022), suggests that ferric iron likely plays an important role in the stability of this phase. It leaves open to question whether jeffbenite inclusions found in superdeep diamonds represent equilibrium conditions of entrapment, or are retrograde.

The high-pressure behavior of jeffbenite synthesized by Smyth et al. (2022) was studied at 300 K by Wang et al. (2021), who reported the high-pressure crystal structure evolution, compressibility, and possible spin state change of iron. Knowledge of the *P-V-T* equation of state for jeffbenite would permit future measurement of the remnant pressure of an inclusion in diamond to estimate its entrapment pressure using inclusion-diamond barometry (e.g., Angel et al., 2022). This paper focuses on determining the *P-V-T* equation of state of ferromagnesian jeffbenite (Mg<sub>2.32</sub>Al<sub>0.03</sub>Fe<sup>2+</sup><sub>1.28</sub>Fe<sup>3+</sup><sub>1.77</sub>Si<sub>2.85</sub>O<sub>12</sub>), which may have a stability field in the transition zone or uppermost lower mantle distinct from majoritic garnet. Results are used to model the potential entrapment pressures of jeffbenite-rich inclusions in diamond.

## 2. Materials and Methods

High-quality single crystals of Al-free, ferromagnesian jeffbenite measuring up to 200 μm in longest dimension were synthesized from a stoichiometric mixture of FeO, Fe<sub>2</sub>O<sub>3</sub>, SiO<sub>2</sub>, MgO and Mg(OH)<sub>2</sub> powders in a multi-anvil press at 15 GPa and 1,200°C at Bayerisches Geoinstitut, University of Bayreuth, Germany. Details of the sample synthesis and compositional characterization are reported in Smyth et al. (2022), including the determination of Fe<sup>3+</sup>/ΣFe = 0.65 (1) by synchrotron Mössbauer spectroscopy. The bulk chemical composition of 34.49 wt% SiO<sub>2</sub>, 18.63 wt% MgO, 44.23 wt% FeO and 0.31 wt% Al<sub>2</sub>O<sub>3</sub> was obtained using a JEOL 8230 electron microprobe at the University of Colorado, and because the H<sub>2</sub>O content was below detection using FTIR spectroscopy, the stoichiometry of this jeffbenite can be written as Mg<sub>2.32</sub>Al<sub>0.03</sub>Fe<sup>2+</sup><sub>1.28</sub>Fe<sup>3+</sup><sub>1.77</sub>Si<sub>2.85</sub>O<sub>12</sub>. Smyth et al. (2022) found the lattice parameters of five crystals from the original batch to be similar, and refined the structure from one in space group *I*-42d with *a* = 6.6449 (3) Å, *c* = 18.4823 (9) Å, and *V* = 816.08 (9) Å<sup>3</sup>. For the high pressure-temperature study, crystals of jeffbenite from the same synthesis run were screened for clean optical extinction under a polarizing-light microscope and polished to ~10 μm thickness.

A BX90-type DAC equipped with 300-μm flat culets diamond anvils was used for high *P-T* measurements with a miniature resistive heater described by Kantor et al. (2012). A gold foil for pressure determination and a polished crystal were loaded together into the sample chamber in a neon pressure medium using the GSECARS gas loading system (Rivers et al., 2008). A closed-loop feedback was used to control the power against the temperature measured at a K-type thermocouple in contact with one of the diamond anvils (Zhang et al., 2022). During the diffraction experiments, the temperature fluctuation was ~1 K at 450 and ~3 K at 750 K. Au foil was used as the pressure calibrant and the pressure uncertainties are ±0.2 GPa or less. *In-situ* high *P-T* single-crystal XRD experiments were conducted up to 33.7 GPa and 750 K at the 13-BM-C experimental station of the Advanced Photon Source, Argonne National Laboratory. The incident X-ray beam at 13 BMC was monochromated to 0.4340 Å with a focal spot size of 12 × 18 μm<sup>2</sup> (Zhang et al., 2017). Data were analyzed by the APEX3 Crystallography Software Suite and SHELXL package (Sheldrick, 2008). *P-V-T* data were fitted by the EoSFit7-GUI program (Gonzalez-Platas et al., 2016). The isomeke *P-T* paths of diamond-jeffbenite pairs were modeled by the EoSFit7Pinc (Angel et al., 2017).

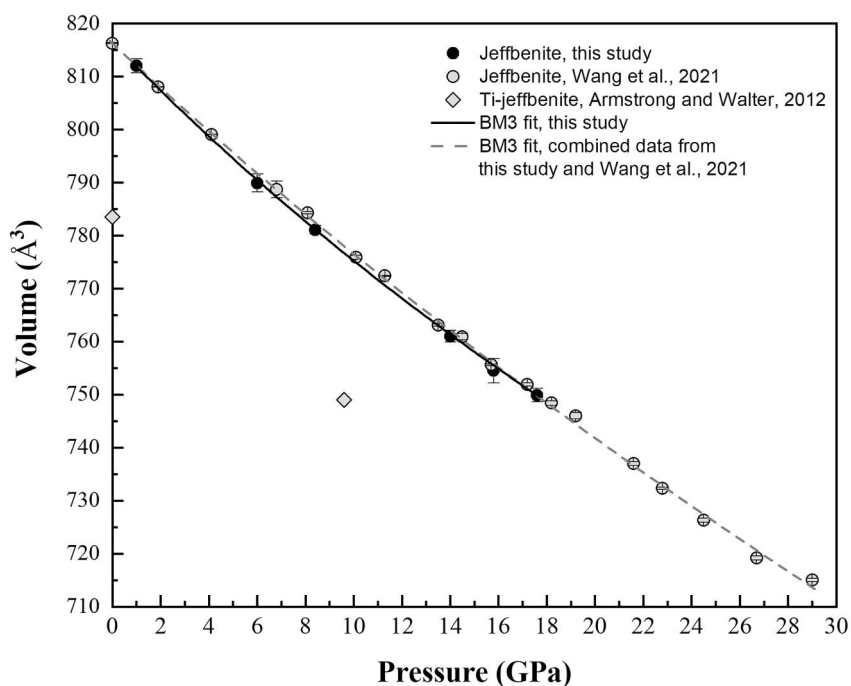


**Figure 1.** 300 K static compression of Fe-jeffbenite from this study and Wang et al. (2021). The two diamond-shaped points represent volumes for Ti-jeffbenite from Armstrong and Walter (2012).

### 3. Results and Discussion

#### 3.1. Isothermal Equation of State at Room-*T*

Lattice parameters and the unit-cell volume of jeffbenite at high-*P* and high-*T* conditions were analyzed using the APEX3 software (Bruker), summarized in Table S1 in Supporting Information S1. There is no indication of phase transition up to 33.7 GPa and 750 K. Additionally, the unit-cell reference volume,  $V_{T0} = 816.5 (1.7) \text{ \AA}^3$ , was obtained prior to compression, which is consistent with previously reported values (Nestola, Prencipe, & Belmonte, 2023; Smyth et al., 2022; Wang et al., 2021). However, the room-*T* volume of  $783.5 (1.3) \text{ \AA}^3$  determined for a synthetic Ti-bearing jeffbenite (Armstrong & Walter, 2012) is significantly lower than Fe-rich jeffbenite in this study.

Because we used the crystals from same synthesis batch as the 300 K static compression data from Wang et al. (2021), those data were incorporated into the *P-V-T* data set and fitted together to a third-order Birch-Murnaghan equation of state (BM3-EoS) using error-weighted least squares with EoSFit7c (Angel et al., 2014). The resulting BM3 parameters are:  $V_{T0} = 816.3 (1) \text{ \AA}^3$ ;  $K_{T0} = 191 (2) \text{ GPa}$ ; and  $K_{T0}' = 2.1 (2)$  (Figure 1, dashed line). The *P-V* data yields values of  $K_{T0} = 171 (1) \text{ GPa}$  when assuming a pressure derivative of  $K_{T0}' \equiv 4$ .

Compared with the room-temperature compression data alone (Wang et al., 2021), the isothermal bulk modulus ( $K_0$ ) of jeffbenite from the combined *P-V-T* EoS is about 5% higher than the value  $K_{T0} = 182 (1) \text{ GPa}$  from Wang et al. (2021). The fitted  $K_{T0}'$  from this *P-V-T* study is somewhat lower than  $K_{T0}' = 2.7 (1)$  from Wang et al. (2021). Nestola, Prencipe, and Belmonte (2023) used first-principles density functional theory (DFT) to calculate the EoS parameters of Mg-jeffbenite and found  $K_{T0} = 175.39 \text{ GPa}$  and  $K_0' = 4.09$ , suggesting that the incorporation of iron may increase the incompressibility of jeffbenite.

The compressibility of pyrope-almandine series garnets using synthetic single-crystal samples show  $K_{T0}$  ranges from  $163.7(1.7)$ – $172.6(1.5) \text{ GPa}$  with  $K_{T0}'$  5.6–6.4 (Milani et al., 2015). For comparison, Zou et al. (2012) measured  $K_0 = 167 (6) \text{ GPa}$  and  $K_0' = 4.6 (3)$  for synthetic  $\text{Mg}_3\text{Al}_2\text{Si}_3\text{O}_{12}$  pyrope garnet. Ismailova et al. (2017) determined the compressibility of majoritic garnets along the  $\text{Fe}_3\text{Al}_2\text{Si}_3\text{O}_{12}$ – $\text{Fe}_4\text{Si}_4\text{O}_{12}$  solid solution containing 23%–76% Fe and found a range in  $K_{T0}$  from 159 (1) to 172 (1) GPa. Compared to our results for jeffbenite with

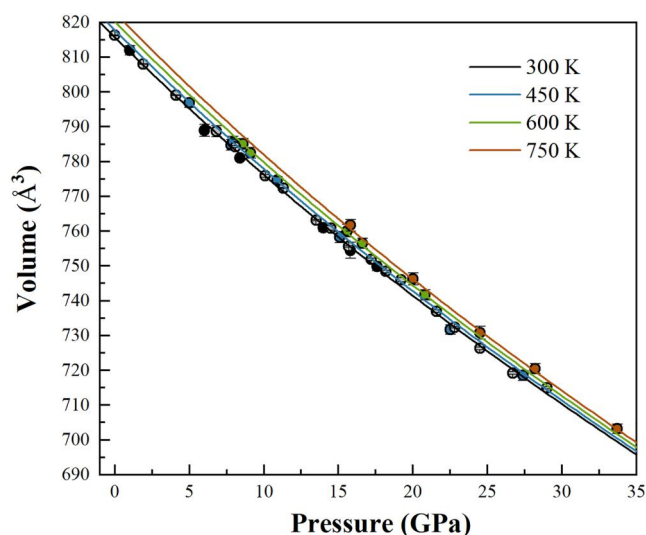


**Figure 2.** Pressure-volume-temperature data for jeffbenite from the current study combined with 300 K compression data on the same material from Wang et al. (2021), shown as gray shaded circles.

Holland & Powell, 2011) (Text S1 in Supporting Information S1). The high  $P$ - $T$  unit-cell volumes for jeffbenite are plotted in Figure 2, together with the isotherms calculated using the thermoelastic parameters derived from the current fits. The  $P$ - $T$  path during data collection is shown in Supplementary Information Figure S1 in Supporting Information S1. The thermoelastic parameters  $(\partial K_{T0}/\partial T)_P$ ,  $\alpha_T$ ,  $K_0$ , and  $K_0'$  obtained in this study with the high-temperature BM3-EoS are:  $V_0 = 815.7$  (2)  $\text{\AA}^3$ ;  $K_0 = 191$  (2) GPa;  $K_0' = 2.0$  (9)  $(\partial K_{T0}/\partial T)_P = -0.0107$  (4) GPa/K; and  $\alpha_T = 3.50$  (3)  $\times 10^{-5}$   $\text{K}^{-1}$ . In addition, by fixing the  $V_0$ ,  $K_0$ , and  $K_0'$  to the values obtained at 300 K, the resulting thermal parameters are  $(\partial K_{T0}/\partial T)_P = -0.0093$  (1) GPa/K, and  $\alpha_T = 3.095$  (1)  $\times 10^{-5}$   $\text{K}^{-1}$ .

Nestola, Prencipe, and Belmonte (2023) also reported the volume thermal expansion coefficient and the temperature derivative of the bulk modulus for pure jeffbenite ( $\text{Mg}_3\text{Al}_2\text{Si}_3\text{O}_{12}$ ) based on ab initio computations, finding  $\alpha_{0V} = 1.717 \times 10^{-5}$   $\text{K}^{-1}$  and  $(\partial K_{T0}/\partial T)_P = -0.020$  GPa/K, respectively. We obtained a larger value for  $\alpha_{0V}$  with a lower temperature derivative of the bulk modulus compared with the computational study of Nestola, Prencipe, and Belmonte (2023) on Mg-jeffbenite without iron.

Du et al. (2015) measured the thermal expansion of pyrope and the derived volume thermal expansivity  $\alpha_{0V}$  is  $2.74$  (5)  $\times 10^{-5}$   $\text{K}^{-1}$ . The thermoelastic parameters of synthetic  $\text{Mg}_3\text{Al}_2\text{Si}_3\text{O}_{12}$  pyrope have also been investigated up to 19 GPa and 1700 K by Zou et al. (2012), who reported  $(\partial K_{T0}/\partial T)_P = -0.021$  (9) GPa/K and  $\alpha_{0V} = 2.89$  (33)  $\times 10^{-5}$   $\text{K}^{-1}$ . Similarly, Wang et al. (1998) found  $(\partial K_{T0}/\partial T)_P = -0.020$  (1) GPa/K and  $\alpha_{0V} = 2.5 \times 10^{-5}$   $\text{K}^{-1}$  for  $\text{Py}_{62}\text{Mj}_{38}$  obtained in multi-anvil apparatus. Our value for the thermal expansion coefficient of jeffbenite is lower than the majoritic garnet with mid-ocean ridge basalt (MORB) composition, with  $\alpha = 2.0$  (3)  $\times 10^{-5}$   $\text{K}^{-1} + T \times 1.0$  (5)  $\times 10^{-8}$   $\text{K}^{-2}$  (Nishihara et al., 2005). However, there is lack thermal expansion data of tetragonal majorite at simultaneous high  $P$ - $T$  conditions for more systematic comparisons. Our fitted values of  $\alpha_{0V}$  and  $(\partial K_{T0}/\partial T)_P$  for Fe-jeffbenite of  $3.095$ – $3.503 \times 10^{-5}$   $\text{K}^{-1}$  and  $-0.01$  GPa/K, respectively, are remarkably different from previous results on majorite-pyrope garnets, further suggesting unique phase space for jeffbenite.

#### 4. Application to Superdeep Diamond

Jeffbenite is a newly named mineral (Nestola et al., 2016) after its discovery as inclusions in super-deep diamond from the Brazil's Juina district and Kankan in Guinea (Brenker et al., 2002; Bulanova et al., 2010; Hayman et al., 2005; Hutchison et al., 2001; Zedgenizov et al., 2020). The jeffbenite-containing diamonds partially overlap with the locations where majorite garnets are also known as inclusions. Using the current thermoelastic results, we calculated the entrapment isomekes for jeffbenite in comparison to majoritic garnet in diamond. Entrapment isomekes give the  $P$  and  $T$  conditions ideally decompressed from the entrapment depth where the pressure on the inclusion is equal to the external pressure on the diamond host, thereby providing a

$K_{T0} = 191$  GPa suggests that jeffbenite is less compressible than all other iron-rich garnets (Table S2 in Supporting Information S1).

As for the high-pressure form of majorite garnet with tetrahedral structure and similar compositions along the majorite-pyrope series, the adiabatic bulk moduli fall in the range from 160 to 173 GPa (Sinogeikin & Bass, 2002; Sinogeikin et al., 1997). Static compression studies of single-crystal majoritic garnet include Yagi et al. (1992) finding  $K_0 = 161.12$  GPa and Hazen et al. (1994) finding  $K_0 = 169.3$  GPa, both for fixed  $K_0' = 4$  and not containing iron (Table S1 in Supporting Information S1). Thus, based on the measurements of adiabatic bulk moduli on majoritic garnet, it is obvious that jeffbenite is less compressible. The higher incompressibility of iron-rich jeffbenite, combined with previous high-pressure structure refinements suggests that  $\text{Fe}^{3+}$  substitution for Si in the tetrahedral site may be a factor in stabilizing jeffbenite at high pressure conditions (Wang et al., 2021).

#### 3.2. Thermal Equation of State of Jeffbenite

Having established a reliable compression curve for jeffbenite at room temperature, we next fitted the thermal equation of state parameters by combining with the Holland Powell-type thermal pressure model, and the temperature derivative of the bulk modulus  $(\partial K_{T0}/\partial T)_P$  (Angel et al., 2014; Fei, 1995;

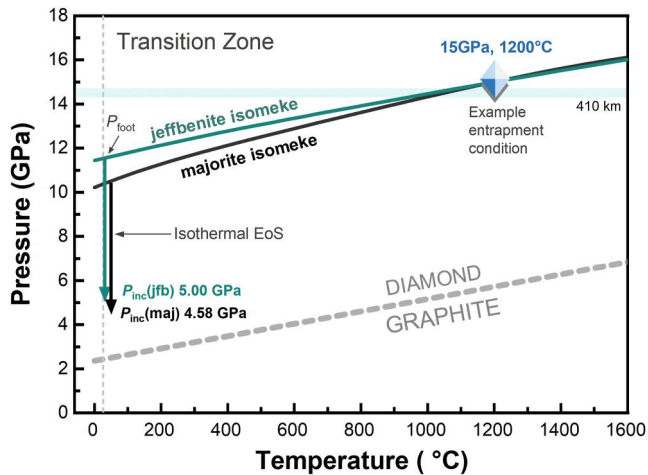


**Figure 3.** Example entrapment isomekes for ferromagnesian jeffbenite and majoritic garnet of MORB composition with a common entrapment pressure of 15 GPa and 1,200°C. The  $P$ - $T$  conditions are calculated using the thermoelastic equation of state for jeffbenite from this study, and from Nishihara et al. (2005) for majoritic garnet. The diamond-graphite equilibrium phase boundary is also shown (Day, 2012). Compared with majoritic garnet, a jeffbenite inclusion entrapped in the mantle transition zone is predicted to exhibit a higher remnant pressure,  $P_{inc}$ .

means to calculate in reverse the possible entrapment depths from the remnant pressure on an inclusion in a diamond at room pressure (Angel et al., 2015, 2017).

Since the remnant pressure on a naturally recovered jeffbenite inclusion has not yet been determined, as an example entrapment isomeke, we will take the mantle transition-zone conditions of synthesis for this material (Smyth et al., 2022) at 15 GPa and 1,200°C as an entrapment condition from which to model the predicted residual pressure of a jeffbenite inclusion ( $P_{inc}$ ) compared with majoritic garnet. Figure 3 presents the example entrapment isomekes for ferromagnesian jeffbenite and majoritic garnet of MORB composition using a hypothetical entrapment condition of 15 GPa and 1,200°C using the  $P$ - $V$ - $T$  equations of state from this study for jeffbenite, and from Nishihara et al. (2005) for majoritic garnet. The differences in the slope for the example entrapment isomeke of jeffbenite and majoritic garnet is due to differences in their thermal expansion coefficients, resulting in different values of  $P_{foot}$ , the isomeke pressure at room temperature. The resulting  $P_{inc}$  values therefore also differ. In our example, the predicted  $P_{foot}$  for jeffbenite is  $\sim 11.5$  GPa, whereas the predicted  $P_{foot}$  for majoritic garnet is  $\sim 1$  GPa lower. Consequently, the calculated  $P_{inc}$  for majoritic garnet found in the same diamond would be lower than that of jeffbenite. Isothermal decompression in our example would lead to a predicted  $P_{inc} = 5.00$  GPa for jeffbenite and 4.58 GPa for majoritic garnet. Although these are relatively high inclusion pressures, they are on the order of what has been observed for in-

clusions entrapped in the mantle transition zone (Genzel et al., 2023). It is possible that jeffbenite and majoritic garnet have overlapping stability fields at transition zone conditions but form under different chemical environments.

Based on our thermoelastic data, if jeffbenite is a retrograde phase from bridgmanite, a volume change about 22% would be required (31.78 g/mol for jeffbenite vs.  $\sim 25$  g/mol for bridgmanite). Such a high-volume change can be accommodated by diamond only within its plastic deformation regime, but more details on fractures and plastic deformation are needed for jeffbenite inclusions to properly estimate the possibility of transformation from bridgmanite to jeffbenite. Nevertheless, our presented thermal EoS still gives a good description of the thermal expansion behavior for jeffbenite over a large temperature and pressure range and could be applied to elastic thermobarometry of diamond-hosted inclusions of jeffbenite in the future.

Jeffbenite inclusions, although rare, can provide direct evidence of super-deep origins of diamonds and the presence of such  $Fe^{3+}$ -rich inclusions may also reflect extreme redox changes during subducted slab dehydration-rehydration processes in the transition zone or uppermost lower mantle (Nestola, Prencipe, & Belmonte, 2023; Tao et al., 2018). Notably, the recently reported high  $Fe^{3+}$  content in majoritic garnet inclusions ( $Fe^{3+}/\sum Fe > \sim 0.81$ ) from the deep upper mantle have raised questions about what controls the redox state in these garnets (Kiseeva et al., 2018; Tao et al., 2018; Xu et al., 2017).

In Fe-jeffbenite, charge balance most likely occurs through the removal of Si on the tetrahedral site to accommodate the additional positive charge, and the excess Si would probably be incorporated into a coexisting phase, such as clinopyroxene in our case (Smyth et al., 2022). Substitution mechanisms such as  $Si^{4+} + Fe^{2+} = 2Fe^{3+}$  suggest that ability for jeffbenite to incorporate  $Fe^{3+}$  may play a potential role in stabilizing it over majoritic garnet. As the oxygen fugacity is above the IW buffer, the high  $Fe^{3+}$  concentration of jeffbenite in the mantle might reflect extreme redox changes (Nestola, Regier, et al., 2023). At some depths, the  $Fe^{3+}$ -jeffbenite inclusions might be a product of a redox reaction involving carbonatitic magmas and carbonates is as the oxidizing agent which responsible for generating the high  $Fe^{3+}$  of these deep mantle inclusions (Lorenzon et al., 2022; Thomson et al., 2016). The question remains, whether or not  $Fe^{3+}$ -jeffbenite is a redox reaction product during diamond formation at different depths in the slab, or whether it possesses a distinct stability field within certain mantle compositions. The abundance of jeffbenite as an inclusion in super-deep diamonds makes determining its primary or retrograde history essential in understanding mantle dynamics.

## 5. Conclusions

The high-pressure high-temperature equation of state of synthetic Fe-jeffbenite was determined by synchrotron-based, single-crystal XRD at pressures up to ~34 GPa and temperatures up to 750 K. The thermoelastic parameters of Fe-jeffbenite are now determined and can be applied to determining entrapment pressures in future finds. Compared with majoritic garnet, the smaller thermal expansivity of jeffbenite likely gives rise to a broader pressure and temperature stability field in the upper lower mantle.

## Data Availability Statement

Data supporting the findings of this study are available at Qin (2023).

## References

- Angel, R. J., Alvaro, M., & Nestola, F. (2022). Crystallographic methods for non-destructive characterization of mineral inclusions in diamonds. *Reviews in Mineralogy and Geochemistry*, 88(1), 257–305. <https://doi.org/10.2138/rmg.2022.88.05>
- Angel, R. J., Alvaro, M., Nestola, F., & Mazzucchelli, M. L. (2015). Diamond thermoelastic properties and implications for determining the pressure of formation of diamond-inclusion systems. *Russian Geology and Geophysics*, 56(1–2), 211–220. <https://doi.org/10.1016/j.rgg.2015.01.014>
- Angel, R. J., Gonzalez-Platas, J., & Alvaro, M. (2014). EosFit7c and a Fortran module (library) for equation of state calculations. *Zeitschrift für Kristallographie*, 229(5), 405–419. <https://doi.org/10.1515/zkri-2013-1711>
- Angel, R. J., Mazzucchelli, M. L., Alvaro, M., & Nestola, F. (2017). A simple GUI for host-inclusion elastic thermobarometry. *American Mineralogist*, 102(9), 1957–1960. <https://doi.org/10.2138/am-2017-6190>
- Armstrong, L. S., & Walter, M. J. (2012). Tetragonal almandine pyrope phase (TAPP): Retrograde Mg-perovskite from subducted oceanic crust? *European Journal of Mineralogy*, 24(4), 587–597. <https://doi.org/10.1127/0935-1221/2012/0024-2211>
- Brenker, F. E., Stachel, T., & Harris, J. W. (2002). Exhumation of lower mantle inclusions in diamond: ATEM investigation of retrograde phase transitions, reactions and exsolution. *Earth and Planetary Science Letters*, 198(1–2), 1–9. [https://doi.org/10.1016/s0012-821x\(02\)00514-9](https://doi.org/10.1016/s0012-821x(02)00514-9)
- Bulanova, G. P., Walter, M. J., Smith, C. B., Kohn, S. C., Armstrong, L. S., Blundy, J., & Gobbo, L. (2010). Mineral inclusions in sublithospheric diamonds from collier 4 kimberlite pipe, Juina, Brazil: Subducted protoliths, carbonated melts and primary kimberlite magmatism. *Contributions to Mineralogy and Petrology*, 160(4), 489–510. <https://doi.org/10.1007/s00410-010-0490-6>
- Day, H. W. (2012). A revised diamond-graphite transition curve. *American Mineralogist*, 97(1), 52–62. <https://doi.org/10.2138/am.2011.3763>
- Du, W., Clark, S. M., & Walker, D. (2015). Thermo-compression of pyrope-grossular garnet solid solutions: Non-linear compositional dependence. *American Mineralogist*, 100(1), 215–222. <https://doi.org/10.2138/am-2015-4752>
- Fei, Y. (1995). Thermal expansion. In T. J. Ahrens (Ed.), *Mineral physics and crystallography: A handbook of physical constants* (pp. 29–44). American Geophysical Union.
- Finger, L. W., & Conrad, P. G. (2000). The crystal structure of “tetragonal almandine-pyrope phase” (TAPP): A reexamination. *American Mineralogist*, 85(11–12), 1804–1807. <https://doi.org/10.2138/am-2000-11-1224>
- Genzel, P. T., Pamato, M. G., Novella, D., Santello, L., Lorenzon, S., Shirey, S. B., et al. (2023). Geobarometric evidence for a LM/TZ origin of CaSiO<sub>3</sub> in a sublithospheric diamond. *Geochemical Perspectives Letters*, 25, 41–45. <https://doi.org/10.7185/geochemlet.2313>
- Gonzalez-Platas, J., Alvaro, M., Nestola, F., & Angel, R. J. (2016). EosFit7-GUI: A new GUI tool for equation of state calculations, analyses, and teaching. *Journal of Applied Crystallography*, 49(4), 1377–1382. <https://doi.org/10.1107/s1600576716008050>
- Harris, J., Hutchison, M. T., Hursthouse, M., Light, M., & Harte, B. (1997). A new tetragonal silicate mineral occurring as inclusions in lower mantle diamonds. *Nature*, 387(6632), 486–488. <https://doi.org/10.1038/387486a0>
- Harte, B. (2010). Diamond formation in the deep mantle: The record of mineral inclusions and their distribution in relation to mantle dehydration zones. *Mineralogical Magazine*, 74(2), 189–215. <https://doi.org/10.1180/minmag.2010.074.2.189>
- Hayman, P. C., Kopylova, M. G., & Kaminsky, F. V. (2005). Lower mantle diamonds from Rio Soriso (Juina area, Mato Grosso, Brazil). *Contributions to Mineralogy and Petrology*, 149(4), 430–445. <https://doi.org/10.1007/s00410-005-0657-8>
- Hazen, R. M., Downs, R. T., Conrad, P. G., Finger, L. W., & Gasparik, T. (1994). Comparative compressibilities of majorite-type garnets. *Physics and Chemistry of Minerals*, 21(5), 344–349. <https://doi.org/10.1007/bf00202099>
- Holland, T. J. B., & Powell, R. (2011). An improved and extended internally consistent thermodynamic dataset for phases of petrological interest, involving a new equation of state for solids. *Journal of Metamorphic Geology*, 29(3), 333–383. <https://doi.org/10.1111/j.1525-1314.2010.00923.x>
- Hutchison, M. T., Hursthouse, M., & Light, M. (2001). Mineral inclusions in diamonds: Associations and chemical distinctions around the 670-km discontinuity. *Contributions to Mineralogy and Petrology*, 142(1), 119–126. <https://doi.org/10.1007/s004100100279>
- Ismailova, L., Bykov, M., Bykova, E., Bobrov, A., Kuppenko, I., Cerantola, V., et al. (2017). Effect of composition on compressibility of skiaegite-Fe-majorite garnet. *American Mineralogist*, 102(1), 184–191. <https://doi.org/10.2138/am-2017-5856>
- Kantor, I., Prakapenka, V., Kantor, A., Dera, P., Kurnosov, A., Sinogeikin, S., et al. (2012). BX90: A new diamond anvil cell design for X-ray diffraction and optical measurements. *Review of Scientific Instruments*, 83(12). <https://doi.org/10.1063/1.4768541>
- Kiseeva, E. S., Vasiukov, D. M., Wood, B. J., McCammon, C., Stachel, T., Bykov, M., et al. (2018). Oxidized iron in garnets from the mantle transition zone. *Nature Geoscience*, 11(2), 144–147. <https://doi.org/10.1038/s41561-017-0055-7>
- Lorenzon, S., Novella, D., Nimis, P., Jacobsen, S. D., Thomassot, E., Pamato, M. G., et al. (2022). Ringwoodite and zirconia inclusions indicate downward travel of super-deep diamonds. *Geology*, 50(9), 996–1000. <https://doi.org/10.1130/g50111.1>
- McCammon, C., Hutchison, M., & Harris, J. (1997). Ferric iron content of mineral inclusions in diamonds from Sao Luiz: A view into the lower mantle. *Science*, 278(5337), 434–436. <https://doi.org/10.1126/science.278.5337.434>
- Milani, S., Nestola, F., Alvaro, M., Pasqual, D., Mazzucchelli, M. L., Domeneghetti, M. C., & Geiger, C. A. (2015). Diamond-garnet geobarometry: The role of garnet compressibility and expansivity. *Lithos*, 227, 140–147. <https://doi.org/10.1016/j.lithos.2015.03.017>
- Nestola, F., Burnham, A. D., Peruzzo, L., Taurom, L., Alvaro, M., Walter, M. J., et al. (2016). Tetragonal almandine pyrope phase, TAPP: Finally a name for it, the new mineral jeffbenite. *Mineralogical Magazine*, 80(7), 1219–1232. <https://doi.org/10.1180/minmag.2016.080.059>

- Nestola, F., Korolev, N., Kopylova, M., Rotiroli, N., Pearson, D. G., Pamato, M. G., et al. (2018). CaSiO<sub>3</sub> perovskite in diamond indicates the recycling of oceanic crust into the lower mantle. *Nature*, 555(7695), 237–241. <https://doi.org/10.1038/nature25972>
- Nestola, F., Prencipe, M., & Belmonte, D. (2023). Mg<sub>3</sub>Al<sub>2</sub>Si<sub>3</sub>O<sub>12</sub> jeffbenite inclusion in super-deep diamonds is thermodynamically stable at very shallow Earth's depths. *Scientific Reports*, 13(1), 1–10. <https://doi.org/10.1038/s41598-022-27290-9>
- Nestola, F., Regier, M. E., Luth, R. W., Pearson, D. G., Stachel, T., McCammon, C., et al. (2023). Extreme redox variations in a superdeep diamond from a subducted slab. *Nature*, 613(7942), 85–89. <https://doi.org/10.1038/s41586-022-05392-8>
- Nishihara, Y., Aoki, I., Takahashi, E., Matsukage, K. N., & Funakoshi, K. I. (2005). Thermal equation of state of majorite with MORB composition. *Physics of the Earth and Planetary Interiors*, 148(1), 73–84. <https://doi.org/10.1016/j.pepi.2004.08.003>
- Pearson, D. G., Brenker, F. E., Nestola, F., McNeill, J., Nasdala, L., Hutchison, M. T., et al. (2014). Hydrous mantle transition zone indicated by ringwoodite included within diamond. *Nature*, 507(7491), 221–224. <https://doi.org/10.1038/nature13080>
- Qin, F. (2023). Data files for thermoelastic properties of Fe<sup>3+</sup>-rich jeffbenite [Dataset]. *Zenodo*. <https://doi.org/10.5281/zenodo.10056631>
- Rivers, M., Prakapenka, V. B., Kubo, A., Pullins, C., Holl, C. M., & Jacobsen, S. D. (2008). The COMPRES/GSECARS gas-loading system for diamond anvil cells at the Advanced Photon Source. *High Pressure Research*, 28(3), 273–292. <https://doi.org/10.1080/08957950802333593>
- Sheldrick, G. M. (2008). A short history of SHELX. *Acta Crystallographica Section A*, 64(Pt 1), 112–122. <https://doi.org/10.1107/s0108767307043930>
- Shirey, S. B., Cartigny, P., Frost, D. J., Keshav, S., Nestola, F., Nimis, P., et al. (2013). Diamonds and the geology of mantle carbon. *Reviews in Mineralogy and Geochemistry*, 75(1), 355–421. <https://doi.org/10.2138/rmg.2013.75.12>
- Sinogeikin, S. V., & Bass, J. D. (2002). Elasticity of majorite and a majorite-pyrope solid solution to high pressure: Implications for the transition zone. *Geophysical Research Letters*, 29(2), 1–4. <https://doi.org/10.1029/2001gl013937>
- Sinogeikin, S. V., Bass, J. D., O'Neill, B., & Gasparik, T. (1997). Elasticity of tetragonal end-member majorite and solid solutions in the system Mg<sub>2</sub>Si<sub>4</sub>O<sub>12</sub>-Mg<sub>3</sub>Al<sub>2</sub>Si<sub>3</sub>O<sub>12</sub>. *Physics and Chemistry of Minerals*, 24(2), 115–121. <https://doi.org/10.1007/s002690050024>
- Smyth, J. R., Wang, F., Alp, E. E., Bell, A. S., Posner, E. S., & Jacobsen, S. D. (2022). Ferromagnesian jeffbenite synthesized at 15 GPa and 1200°C. *American Mineralogist: Journal of Earth and Planetary Materials*, 107(3), 405–412. <https://doi.org/10.2138/am-2021-7852>
- Stachel, T., Brey, G. P., & Harris, J. W. (2005). Inclusions in sublithospheric diamonds: Glimpses of deep Earth. *Elements*, 1(2), 73–78. <https://doi.org/10.21113/gselements.1.2.73>
- Tao, R. B., Fei, Y. W., Bullock, E. S., Xu, C., & Zhang, L. F. (2018). Experimental investigation of Fe<sup>3+</sup>-rich majoritic garnet and its effect on majorite geobarometer. *Geochimica et Cosmochimica Acta*, 225, 1–16. <https://doi.org/10.1016/j.gca.2018.01.008>
- Thomson, A. R., Walter, M. J., Kohn, S. C., & Brooker, R. A. (2016). Slab melting as a barrier to deep carbon subduction. *Nature*, 529(7584), 76–79. <https://doi.org/10.1038/nature16174>
- Walter, M. J., Bulanova, G. P., Armstrong, L. S., Keshav, S., Blundy, J. D., Gudfinnsson, G., et al. (2008). Primary carbonatite melt from deeply subducted oceanic crust. *Nature*, 454(7204), 622–625. <https://doi.org/10.1038/nature07132>
- Walter, M. J., Kohn, S. C., Araujo, D., Bulanova, G. P., Smith, C. B., Gaillou, E., et al. (2011). Deep mantle cycling of oceanic crust: Evidence from diamonds and their mineral inclusions. *Science*, 334(6052), 54–57. <https://doi.org/10.1126/science.1209300>
- Wang, F., Thompson, E. C., Zhang, D., Alp, E. E., Zhao, J., Smyth, J. R., & Jacobsen, S. D. (2021). High-pressure crystal structure and equation of state of ferromagnesian jeffbenite: Implications for stability in the transition zone and uppermost lower mantle. *Contributions to Mineralogy and Petrology*, 176(11), 1–13. <https://doi.org/10.1007/s00410-021-01850-0>
- Wang, Y., Weidner, D. J., Zhang, J., Gwanmesia, G. D., & Liebermann, R. C. (1998). Thermal equation of state of garnets along the pyrope-majorite join. *Physics of the Earth and Planetary Interiors*, 105(1–2), 59–71. [https://doi.org/10.1016/s0031-9201\(97\)00072-1](https://doi.org/10.1016/s0031-9201(97)00072-1)
- Xu, C., Kynický, J., Tao, R., Liu, X., Zhang, L., Pohanka, M., et al. (2017). Recovery of an oxidized majorite inclusion from Earth's deep asthenosphere. *Science Advances*, 3(4), e1601589. <https://doi.org/10.1126/sciadv.1601589>
- Yagi, T., Uchiyama, Y., Akaogi, M., & Ito, E. (1992). Isothermal compression curve of MgSiO<sub>3</sub> tetragonal garnet. *Physics of the Earth and Planetary Interiors*, 74(1–2), 1–7. [https://doi.org/10.1016/0031-9201\(92\)90063-2](https://doi.org/10.1016/0031-9201(92)90063-2)
- Zedgenizov, D. A., Kagi, H., Ohtani, E., Tsujimori, T., & Komatsu, K. (2020). Retrograde phases of former bridgmanite inclusions in superdeep diamonds. *Lithos*, 370, 105659. <https://doi.org/10.1016/j.lithos.2020.105659>
- Zedgenizov, D. A., Kagi, H., Shatsky, V. S., & Ragozin, A. L. (2014). Local variations of carbon isotope composition in diamonds from Sao-Luis (Brazil): Evidence for heterogenous carbon reservoir in sublithospheric mantle. *Chemical Geology*, 363, 114–124. <https://doi.org/10.1016/j.chemgeo.2013.10.033>
- Zhang, D., Dera, P. K., Eng, P. J., Stubbs, J. E., Zhang, J. S., Prakapenka, V. B., & Rivers, M. L. (2017). High pressure single crystal diffraction at PX<sup>2</sup> JoVE. *Journal of Visualized Experiments*(119), e54660. <https://doi.org/10.3791/54660-v>
- Zhang, D., Xu, J., Dera, P. K., Rivers, M. L., Eng, P. J., Prakapenka, V. B., & Stubbs, J. E. (2022). Recent developments on high-pressure single-crystal X-ray diffraction at the Partnership for eXtreme Xtallography (PX<sup>2</sup>) program. *Physics and Chemistry of Minerals*, 49(6), 19. <https://doi.org/10.1007/s00269-022-01197-3>
- Zou, Y. T., Gréaux, S., Irifune, T., Whitaker, M. L., Shinmei, T., & Higo, Y. (2012). Thermal equation of state of Mg<sub>3</sub>Al<sub>2</sub>Si<sub>3</sub>O<sub>12</sub> pyrope garnet up to 19 GPa and 1700 K. *Physics and Chemistry of Minerals*, 39(7), 589–598. <https://doi.org/10.1007/s00269-012-0514-z>